Chapter 3
Photovoltaic Source Models

3.1 Introduction

Nowadays, the more and more growing interest in applications of photovoltaic (PV) generation, with all the related problems of optimal exploitation, environmental impact, and grid stability, has determined a speedup of the research in this field. In particular, several issues are currently under consideration such as the prediction of PV energy production, the optimal choice and design of the power converters interfacing the PV generator to utility or load, and the study of all the problems related to the power electronic control. In order to suitably face these problems, an accurate modeling of the PV source is necessary. As a matter of fact, such modeling allows the electrical characteristics of a PV source to be defined, for varying load and environmental conditions, so to obtain an evaluation of the PV source behavior in any operating condition.

The mathematical model of a PV source is, therefore, useful when dealing with dynamic analysis of power converters, assessing the most suitable maximum power point tracking (MPPT) algorithms and, above all, when developing simulations tools for PV systems, either at software or hardware level. Some terms used, henceforth, need an explanation. A PV source is in general a device converting the light of sun into electricity. The elementary PV source is the PV *cell*. A device formed of series/parallel connected PV cells is called PV *module*. Generally, the PV *module* is the basic element of larger PV systems. A PV *field* may be either a module or a set of series/parallel connected modules.

Summarizing the contents of this chapter, the fundamentals of PV sources modeling are given, starting from the static double diode model of a PV cell up to the simplified single diode representation of a PV field, including parasitic and nonideality effects, obtained under uniform illumination. This last model will be used in the following for further investigations on the PV system emulation.

The dynamic model of a PV source is then described. Furthermore, some solutions to extend the modeling to the case of nonuniform solar irradiance are outlined too.

M. C. Di Piazza and G. Vitale, *Photovoltaic Sources*, Green Energy and Technology,
DOI: 10.1007/978-1-4471-4378-9_3, © Springer-Verlag London 2013

3.2 Static Model

3.2.1 Circuit Model of a PV Cell

A mathematical expression of the current/voltage (*I–V*) terminal characteristics for PV cells, coming from the theory of semiconductors, has been described in Chap. 2, Sect. 2.13.4.

The basic equation that analytically describes the *I–V* characteristic of the ideal PV cell is derived by the solutions of the minority carrier diffusion equations. In particular, these solutions can be used to evaluate the minority carrier current densities equations, as shown in Chap. 2. Introducing these last equations in the expression of the PV cell total current, the following relationship is obtained:

$$I = I_{\text{ph}} - I_{s1}(e^{qV/kT} - 1) - I_{s2}(e^{qV/2kT} - 1) \tag{3.1}$$

where:

I is the PV cell terminal current
V is the PV cell terminal voltage
k is the Boltzman constant $= 1.38 \times 10^{-23}$ J/K
q is the electronic charge $= 1.6 \times 10^{-19}$ C
T is the PV cell temperature
I_{s1} is the dark saturation current due to recombination in the quasi-neutral region (diffusion)
I_{s2} is the dark saturation current due to recombination in the space charge region
I_{ph} is the photo-generated current, linearly depending on solar irradiance

The photo-generated current and the dark saturation currents are given by rather complicated expressions depending on the cell structure, material properties, and operating conditions, as described in Chap. 2.

An in-depth understanding of the PV cell operation requires a detailed study of these terms. On the other hand, the basic form of Eq. (3.1) gives important information about the cell's behavior.

From a circuit point of view, Eq. (3.1) can be considered as a Kirchhoff current law; it shows that a PV cell can be modeled as an ideal current source in parallel with two diodes, reflecting the physical behavior of the *p-n* junction.

The first diode has an unitary ideality factor, whereas an ideality factor equal to two is assigned to the second diode as exhibited by denominators of the exponentials in Eq. (3.1).

Figure 3.1 shows the circuit model of a PV cell where the whole current flowing through the diodes is:

$$I_d = I_{d1} + I_{d2} = I_{s1}(e^{qV/kT} - 1) + I_{s2}(e^{qV/2kT} - 1) \tag{3.2}$$

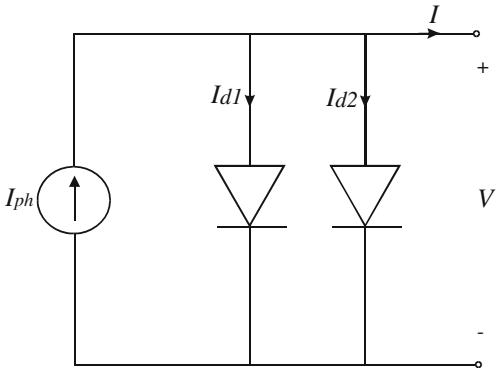

Fig. 3.1 PV cell circuit model

The PV cell circuit model is based on the assumption of linearity, i.e., the assumption that the current flowing through the PV cell is the superposition of two currents, one due to the junction bias, and the other due to illumination.

From this assumption, it is possible to obtain the PV cell I–V characteristic according to the composition schematized in Fig. 3.2. Considering that the current generator and the diode are parallel connected, the I–V curve is obtained by algebraically summing, point-by-point, the devices current having the same voltage.

From the I–V curve shape it is possible to assess that a PV cell, especially if a practical device is considered, can be regarded as an hybrid current–voltage source depending on the operating point. In particular, two regions can be distinguished on the I–V curve, namely a nearly constant current region and a nearly constant voltage region. These regions will be referred, hereinafter, as constant current region and constant voltage region, for convenience.

Once the electrical characteristic of a PV cell is derived, some remarkable points associated to the PV cell behavior can be defined. They are: the *short-circuit current point*, the *open circuit voltage point*, and the *maximum power point*. As well as the above cited points, an important parameter relevant to the PV cell efficiency to be defined is the *fill factor*.

3.2.1.1 Short-Circuit Current

If the PV source is connected to a load with low impedance, nearly all the photo-generated current flows through the load, the diodes are not biased and the voltage at the PV source terminals is near to zero. In this case, the terminal current equals the photo-generated current that is well approximated by the short-circuit current I_{sc}, i.e., the terminal current for $V = 0$. I_{sc} is, therefore, the ordinate of the point of the PV cell characteristic intersecting the I-axis.

The short-circuit current in a PV cell is proportional to the solar irradiance, for a wide range of cell design and irradiance values, provided that the temperature of

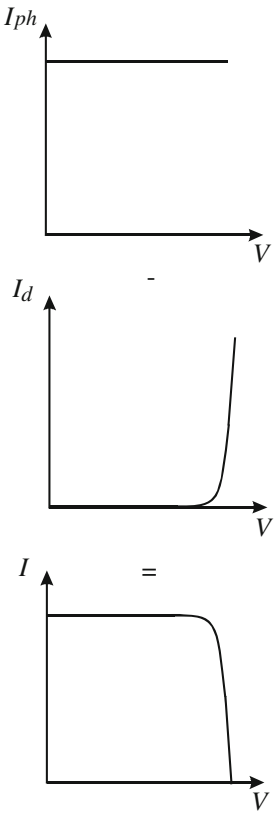

Fig. 3.2 I–V characteristic of the PV cell, obtained by composition of photo generated and diode currents

the cell is the same and that the PV cell does not receive high irradiance values, as in the case of concentrating PV systems.

In a practical PV device, datasheets only provide the nominal short-circuit current, which is the maximum current available at the terminals of the device for a given solar irradiance.

Even if in many cases the assumption of the independence of the short-circuit current on temperature is acceptable, according to literature it can be removed introducing a temperature coefficient for the short-circuit current. For a silicon PV cell, a typical value of 6.4×10^{-6} A/cm^2 °C is frequently used.

3.2.1.2 Open Circuit Voltage

When the PV source is connected to a load with high impedance, nearly all the photo-generated current flows through the diodes, the diodes are directly biased and the PV cell terminal current drops rapidly up to the open circuit condition $I = 0$.

When the open circuit condition is reached, all the photo-generated current is flowing through diodes, thus, considering that $I_{ph} \approx I_{sc}$, the open circuit voltage V_{oc}, can be expressed as:

$$V_{oc} = \frac{2}{3}\frac{kT}{q}\ln\left(\frac{I_{sc} + I_{d1} + I_{d2}}{I_{d1}I_{d2}}\right) \approx \frac{2}{3}\frac{kT}{q}\ln\left(\frac{I_{sc}}{I_{d1}I_{d2}}\right) \tag{3.3}$$

since $I_{sc} \gg I_{d1} + I_{d2}$.

Equation (3.3) demonstrates that the value of the open circuit voltage depends on the logarithm of $I_{sc}/I_{d1}I_{d2}$. Therefore, provided that the cell temperature is constant, the open circuit voltage values scale logarithmically with the short-circuit current which, in turn shows a linear dependence on solar irradiance. This means that the open circuit voltage has a logarithmic dependence on solar irradiance. As a result, it is possible to assess that solar irradiance has a much larger effect of on short-circuit current than on open circuit voltage.

On the other hand, a temperature effect on the open circuit voltage is noticeable. In particular, for typical silicon PV cells in a wide range of operating temperatures, a linear dependence of V_{oc} on T is observed with a temperature coefficient of about −2.3 mV/ °C.

3.2.1.3 Maximum Power Point

The power generated by a PV cell is expressed by the product of the terminal voltage and current. This output power is zero both at the short circuit and open voltage points since the output voltage and the output current are zero, respectively, in these two cases. Between these two extreme points, the power generated by the PV cell is positive.

A remarkable point of the PV cell electrical characteristic is the point where the produced power is at a maximum. This point is referred as maximum power point (MPP) and the corresponding voltage and current are indicated as V_{MP} and I_{MP}, as a rule.

Figure 3.3 shows the PV cell I–V characteristic with the short circuit, open voltage and maximum power points highlighted. As depicted in Fig. 3.3, the MPP defines the rectangle whose area, $P_{MP} = V_{MP}I_{MP}$, is the largest obtainable for any I–V couple on the cell characteristic. The coordinates of the V_{MP} are found by solving the following equation:

$$\left.\frac{dP}{dV}\right|_{V=V_{MP}} = \left.\frac{d(IV)}{dV}\right|_{V=V_{MP}} = \left.\left(I + V\frac{dI}{dV}\right)\right|_{V=V_{MP}} = 0 \tag{3.4}$$

then I_{MP} is determined by evaluating Eq. (3.1) at $V = V_{MP}$.

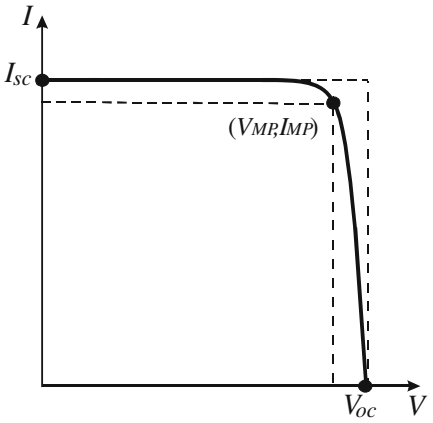

Fig. 3.3 I–V characteristic of the PV cell with remarkable points highlighted

3.2.1.4 Fill Factor

The fill factor (FF) of a PV cell is an important figure of merit whose meaning is relevant to the cell efficiency. It is defined as the ratio between the maximum power $P_{\mathrm{MP}} = I_{\mathrm{MP}}V_{\mathrm{MP}}$, and the product $I_{\mathrm{sc}}V_{\mathrm{oc}}$, as expressed in Eq. (3.5).

$$FF = \frac{P_{\mathrm{MP}}}{I_{\mathrm{sc}}V_{\mathrm{oc}}} = \frac{I_{\mathrm{MP}}V_{\mathrm{MP}}}{I_{\mathrm{sc}}V_{\mathrm{oc}}} \tag{3.5}$$

The FF is a measure of the squareness, in a word of the ideality, of the PV cell *I–V* characteristic; in particular, it represents the ratio between the areas of the rectangles highlighted in Fig. 3.3.

The literature gives an approximation of the FF by the following empirical expression:

$$FF = \frac{V_{\mathrm{oc}} - \frac{kT}{q}\ln(qV_{\mathrm{oc}}/kT + 0.72)}{V_{\mathrm{oc}} + kT/q} \tag{3.6}$$

The relationship between the FF and the PV cell efficiency η is:

$$\eta = \frac{P_{\mathrm{MP}}}{P_i} = FF\frac{I_{\mathrm{sc}}V_{\mathrm{oc}}}{P_i} \tag{3.7}$$

where P_i is the power incident on the PV cell, whose value is tied to the characteristic of the light spectrum hitting the PV cell. Therefore, the closer the FF is to one the higher will be the cell efficiency. In the ideal case FF = 1.

3.2.2 Diffusion Diode Non-Ideality

In the mathematical model of the PV cell expressed by Eq. (3.1), a unitary ideality factor of the diffusion diode has been assigned.

In a practical device, a *I–V* characteristic with ideality factor equal to 1 is unlikely. Therefore, an additional parameter A_0 is usually introduced in the PV cell *I–V* equation to take into account the nonidealities in the junction behavior. With this assumption, Eq. (3.1) can be reformulated as follows:

$$I = I_{\text{ph}} - I_{s1}(e^{qV/A_0kT} - 1) - I_{s2}(e^{qV/2kT} - 1) \tag{3.8}$$

3.2.3 Parasitic Resistance Effects

In the operation of a practical PV cell several phenomena, affecting the cell response, occur. Most of these effects have not been modeled until now, since the solar cell has been described as a nearly ideal device.

It should be observed that, for an accurate representation of the PV cell electrical behavior, the cited effects should be taken into account.

First of all the so-called parasitic resistance effects have to be introduced in the model. In particular, two resistive terms have to be accounted for: the series resistance and the shunt resistance.

3.2.3.1 Series Resistance

The series resistance R_s in a PV cell is a lumped element used to model the series power losses due to the current circulation through different parts of the device. It can be placed between the cathode of the diodes and the corresponding output terminal.

R_s results from the sum of several structural resistances. It mainly depends on the contact of the metal base with the *p*-doped semiconductor layer, the resistance of the base and emitter layers, the contact resistance of the *n*-doped layer with the top metal grid, the resistance of the grid, and other contact resistances.

The effect of the series resistance on the PV cell I–V curve is represented in Fig. 3.4. A quantitative evaluation of this effect is given in Sect. 5.4.2.

It should be observed that R_s has a stronger influence on the part of the electrical characteristic at the right of the MPP, i.e., the constant voltage region. Moreover, it has no effect on the open circuit voltage, whereas it lessens the short-circuit current.

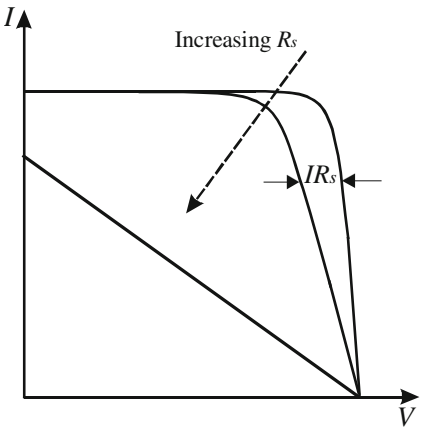

Fig. 3.4 Effect of the series resistance on the I–V characteristic

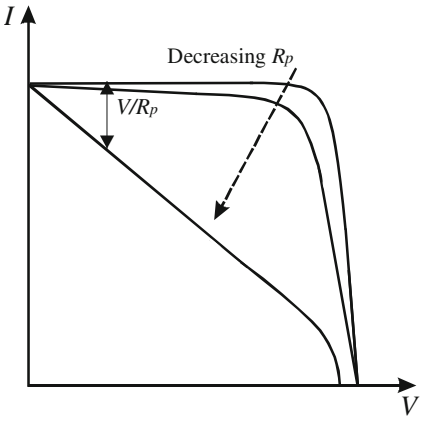

Fig. 3.5 Effect of the shunt resistance on the I–V characteristic

3.2.3.2 Shunt Resistance

The shunt resistance R_p in a PV cell is a lumped element used to model the effects of leakage currents of the *p-n* junction. It can be placed in parallel with the diodes.

Several shunt resistive losses are found in a practical PV device, for example local short circuits in the emitter layer or perimeter shunts along the semiconductor borders. Therefore, R_p mainly depends on the fabrication process of the PV cell.

The effect of the shunt resistance on the PV cell *I–V* curve is represented in Fig. 3.5. A quantitative evaluation of this effect is given in Sect. 5.4.2.

The shunt resistance has a stronger influence on the part of the electrical characteristic at the left of the MPP, i.e., the constant current region. Furthermore, it has no effect on the short-circuit current, whereas it affects the open circuit voltage.

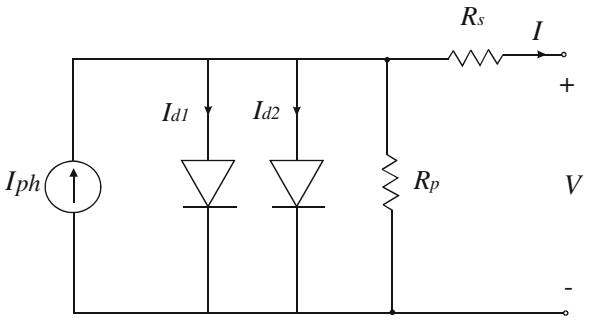

Fig. 3.6 Circuit model of a practical PV cell including series and shunt parasitic resistances

3.2.4 Generalized Double Diode Model

The circuit model referred to a practical PV cell, including the parasitic resistances, is shown in Fig. 3.6.

The corresponding equation, taking into account the nonideality of the diffusion diode as well, is:

$$I = I_{\text{ph}} - I_{s1}(e^{q(V+IR_s)/A_0kT} - 1) - I_{s2}(e^{q(V+IR_s)/2kT} - 1) - \frac{(V + IR_s)}{R_p} \qquad (3.9)$$

Equation (3.9) represents the generalized double diode mathematical model of a real PV cell.

The double diode or double exponential model of a PV cell is generally accepted as reflecting the electrical behavior of real PV cells, especially those constructed from polycrystalline silicon. This representation of solar cell behavior, incorporating the space charge recombination effects by a separate current component with its own exponential voltage dependence, is considered by the literature as the most accurate, especially when dealing with low illuminations. This consideration is important when modeling is oriented to the optimization of solar cells manufacturing processes.

On the other hand, when the study is focused on a PV modules or fields, the implications of low irradiance are less important since the PV electric power generation occurs at high irradiance values.

In the following subsection the simplified single diode representation, which is the most commonly used when the PV modeling is aimed to power generation issues, is given.

3.2.5 Simplified Single Diode Model

The single diode model is a simplified representation of the PV cell *I–V* characteristic. It is derived from the Shockley diode equation including a diode quality

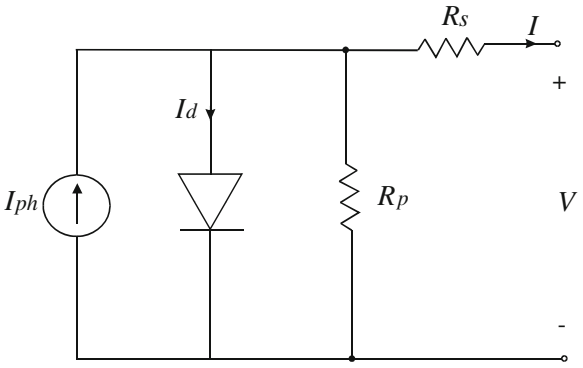

Fig. 3.7 Single diode circuit model of a practical PV cell

factor A_q to approximate the effect of both diffusion and recombination in the space charge layer.

3.2.5.1 The Shockley Diode Equation

The Shockley diode equation relates the current of a *p-n* junction diode, I_D to the diode voltage V_D, according to the so-called *I–V* characteristic:

$$I_D = I_s(e^{V_D/A_q V_T} - 1) \tag{3.10}$$

where I_s is the saturation current or scale current of the diode, $V_T = kT/q$ is the thermal voltage, and A_q is the diode ideality factor.

Equation (3.10) can be regarded as equivalent to Eq. (2.78) but, in this case, the dependence on the fabrication process and on the semiconductor material is considered by introducing the ideality factor of the diode.

A_q varies from 1 to 2; in particular, $A_q \approx 1$ for diodes dominated by the recombination in quasi-neutral region and $A_q \approx 2$ for diodes dominated by the recombination in the depletion region.

3.2.5.2 PV Cell Single Diode Equivalent Circuit

On the basis of the Shockley diode representation, the *I–V* equation of the PV cell becomes:

$$I = I_{\text{ph}} - I_s(e^{q(V+IR_s)/A_q kT} - 1) - \frac{(V + IR_s)}{R_p} \tag{3.11}$$

The corresponding equivalent circuit is that sketched in Fig. 3.7.

The obtained model is quite general, it can be used for different solar cells where the parameters represent physical phenomena of the source. For example, in case of organic cells (see Sect. 2.15.5), the current source I_{ph} corresponds to the

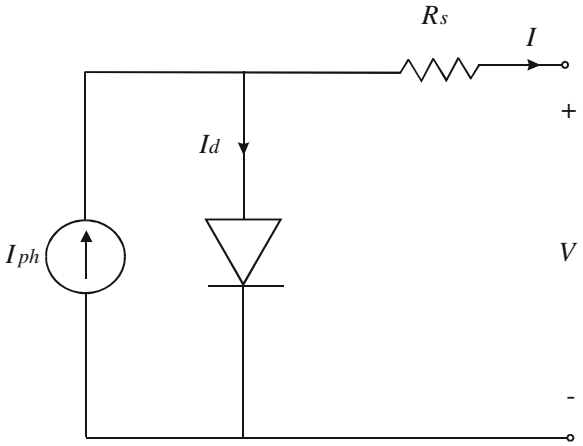

Fig. 3.8 Simplified single diode circuit model of a practical PV cell

number of free electrons/holes pairs after generation and before any recombination process, the shunt resistor R_p is due to the recombination at the interface between the donor and the acceptor material, and may include other recombination effects far away from the dissociation site, the series resistor R_s considers conductivity of each carrier in the transport medium and it is affected by space charges and traps.

If the shunt resistor R_p can be neglected, the last term in Eq. (3.11) is null and the so called four parameter model, given by Eq. (3.12), is obtained.

$$I = I_{\text{ph}} - I_s(e^{q(V+IR_s)/A_qkT} - 1) \tag{3.12}$$

On the basis of such a simplification, a final simplified single diode equivalent circuit is derived. This equivalent circuit is shown in Fig. 3.8; it will be considered as the reference model both for the simulated analysis of the PV system and for the set up of the PV source emulator henceforth.

As previously explained, the presence of the shunt resistor in the circuit model is mainly due to the leakage current of the *p-n* junction depending on the fabrication process of the PV cell. Considering PV modules or fields as a part of an electric generation system, the shunt resistance has a stronger influence in an uncommon region of operation, i.e., the constant current region and for low solar irradiance values. Therefore, the simplification introduced by neglecting R_p does not affect significantly the validity of the model and its use for the scope of emulating the PV source, since the power generation occurs at high irradiance values and in the neighborhood of the MPP. This can be deduced by the example shown in Fig. 5.18.

It is a common practice to neglect the term '–1' in Eq. (3.12) because, in silicon devices, the dark saturation current is much smaller than the exponential term. With this further assumption, the final PV cell model formulation is:

$$I = I_0 - e^{[(V+IR_s)K_1+K_2]} \tag{3.13}$$

with the positions:

$$\begin{aligned} I_{\text{ph}} &= I_0 \\ \frac{q}{A_q kT} &= K_1 \\ I_s &= e^{K_2} \end{aligned} \tag{3.14}$$

Using Eqs. (3.13) and (3.14), the PV cell electrical behavior can be studied once the four model parameters K_1, K_2, R_s, and I_0 are known.

3.2.5.3 PV Voltage versus Current Model Explicit Formulation

The PV model inversion, i.e., the model representation as $V = f(I)$, is particularly useful for the source emulation purpose. As a matter of fact, it is convenient to obtain the voltage on the basis of the actual current, as it will be explained in detail in the chapters dedicated to emulation.

When the single diode model neglecting R_p is considered, the analytical solution of the equation $V = f(I)$ is straightforward. In particular, this solution is obtained by the inversion of Eq. (3.12) in which the dark saturation current is neglected respect to the exponential term or by the inversion of Eq. (3.13).

The following equations are obtained, respectively:

$$V = \frac{A_q kT}{q} \ln\left(\frac{I_{\text{ph}} - I}{I_s}\right) - IR_s \tag{3.15}$$

$$V = \frac{\ln(I_0 - I) - K_2}{K_1} - IR_s \tag{3.15a}$$

It should be observed that the logarithmic term is null for $I = I_{\text{ph}} - I_s$ and it becomes negative for $I_{\text{ph}} - I_s < I < I_{\text{ph}}$. Since I_s is much smaller than the other currents, it is necessary to put particular care to acquire experimental values of current near to the short-circuit condition because the presence of a superimposed noise could result in a negative voltage value or a calculation error evaluating the logarithm.

When the considered PV model is that described in Eq. (3.11), the inversion is more complex and can be managed using the Lambert W function.

The Lambert W function is defined to be the multivalued inverse of the function $f(w) = we^w$.

For our purpose, the attention can be focused on the real-valued Lambert W$(f(w))$, then the relation is defined only for $f(w) \geq -1/e$. If the equation is written under the form $Y = Xe^X$, the X value is obtained as $X =$ Lambert W(Y).

In Fig. 3.9 the real branch of the Lambert W function for $x > -1/e$ is plotted, according to the following Matlab® commands:

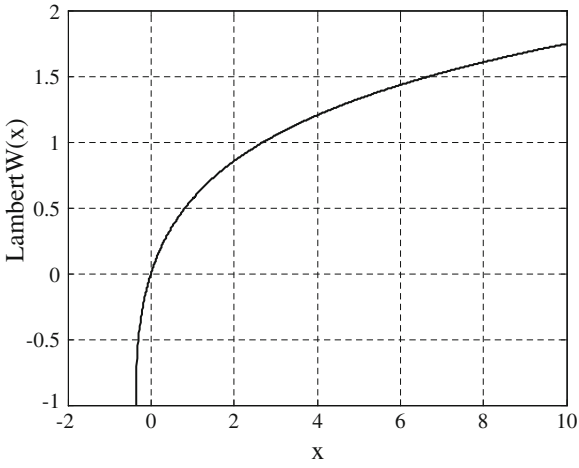

Fig. 3.9 Real branch of the Lambert W function

$\gg x = (-1/2.7183{:}0.01{:}10)$;
$\gg L = lambertw(x)$;
$\gg plot(x, L)$;

On this basis, the following explicit expressions of $V = f(I)$ are obtained:

$$V = -IR_s + \left(A_q V_T\right) \ln\left(\frac{A_q V_T}{I_s R_p} \text{Lambert } W\left\{\frac{I_s R_p}{A_q V_T} \exp\left[\frac{R_p}{A_q V_T}\left(I_{\text{ph}} - I + I_s\right)\right]\right\}\right) \tag{3.16}$$

$$V = I\left(R_p + R_s\right) - I_{ph} R_p + I_s R_p - \left(A_q V_T\right) \text{Lambert } W\left\{\frac{I_s R_p}{A_q V_T} \exp\left[\frac{R_p}{A_q V_T}\left(I_{\text{ph}} - I + I_s\right)\right]\right\} \tag{3.17}$$

The demonstration of (3.16) and (3.17) are given in the next section "Calculus of $I = f(V)$ by Lambert W Function".

3.2.5.4 Calculus of $V = f(I)$ by Lambert W Function

Equation (3.11) can be rewritten as:

$$I = I_{\text{ph}} - I_s\left(e^{\frac{V+IR_s}{A_q V_T}} - 1\right) - \frac{(V + IR_s)}{R_p} \tag{3.18}$$

where $V_T = \frac{kT}{q}$

$$I_{\text{ph}} - I + I_s = I_s e^{\frac{V+IR_s}{A_q V_T}} + \frac{(V + IR_s)}{R_p} \tag{3.19}$$

multiplying both member for $\frac{R_p}{A_q V_T}$

$$\frac{R_p}{A_q V_T}\left(I_{ph} - I + I_s\right) = \frac{R_p I_s}{A_q V_T} e^{\frac{V+IR_s}{A_q V_T}} + \frac{(V + IR_s)}{A_q V_T} \tag{3.20}$$

taking the exponential of both members

$$\exp\left[\frac{R_p}{A_q V_T}\left(I_{\text{ph}} - I + I_s\right)\right] = \exp\left[\frac{R_p I_s}{A_q V_T} e^{\frac{V+IR_s}{A_q V_T}}\right] \cdot \exp\left[\frac{(V + IR_s)}{A_q V_T}\right] \tag{3.21}$$

multiplying both member for $\frac{I_s R_p}{A_q V_T}$

$$\frac{I_s R_p}{A_q V_T}\exp\left[\frac{R_p}{A_q V_T}\left(I_{\text{ph}} - I + I_s\right)\right] = \frac{I_s R_p}{A_q V_T} e^{\frac{V+IR_s}{A_q V_T}} \cdot \exp\left[\frac{R_p I_s}{A_q V_T} e^{\frac{V+IR_s}{A_q V_T}}\right] \tag{3.22}$$

It should be noted that the second member of Eq. (3.22) is in the form we^w where:

$$w = \frac{I_s R_p}{A_q V_T} e^{\frac{V+IR_s}{A_q V_T}} \tag{3.22a}$$

Finally, the Lambert W function can be applied to both members

$$\text{Lambert } W\left\{\frac{I_s R_p}{A_q V_T}\exp\left[\frac{R_p}{A_q V_T}\left(I_{\text{ph}} - I + I_s\right)\right]\right\} = \frac{I_s R_p}{A_q V_T} e^{\frac{V+IR_s}{A_q V_T}} \tag{3.23}$$

and the $V = f(I)$ formulation is obtained as:

$$V = -IR_s + \left(A_q V_T\right)\ln\left(\frac{A_q V_T}{I_s R_p}\text{Lambert } W\left\{\frac{I_s R_p}{A_q V_T}\exp\left[\frac{R_p}{A_q V_T}\left(I_{\text{ph}} - I + I_s\right)\right]\right\}\right) \tag{3.24}$$

or by using Eq. (3.18) as:

$$I_s R_p e^{\frac{V+IR_s}{A_q V_T}} = -I\left(R_p + R_s\right) + I_{\text{ph}} R_p - I_s R_p - V \tag{3.25}$$

$$\begin{aligned} &-I\left(R_p + R_s\right) + I_{ph} R_p - I_s R_p - V = \\ &\left(A_q V_T\right)\text{Lambert } W\left\{\frac{I_s R_p}{A_q V_T}\exp\left[\frac{R_p}{A_q V_T}\left(I_{\text{ph}} - I + I_s\right)\right]\right\} \end{aligned} \tag{3.26}$$

$$\begin{aligned} V = {} & I\left(R_p + R_s\right) - I_{ph} R_p + I_s R_p \\ & - \left(A_q V_T\right)\text{Lambert } W\left\{\frac{I_s R_p}{A_q V_T}\exp\left[\frac{R_p}{A_q V_T}\left(I_{\text{ph}} - I + I_s\right)\right]\right\} \end{aligned} \tag{3.27}$$

3.2.5.5 PV Current versus Voltage Model Explicit Formulation

The Lambert W function can be used to express I versus V as an explicit function, as well. In this case, the following expression is obtained:

$$I = \frac{A_q V_T}{R_s} \text{Lambert } W\left[\frac{I_s R_p R_s}{A_q V_T (R_s + R_p)} \exp\left(\frac{R_p (I_{ph} R_s + I_s R_s + V)}{A_q V_T (R_s + R_p)}\right)\right] + \frac{V - (I_{\text{ph}} - I_s) R_p}{R_s + R_p} \tag{3.28}$$

The demonstration of Eq. (3.28) is given in the next section "Calculus of $I = f(V)$ by Lambert W Function".

3.2.5.6 Calculus of $I = f(V)$ by Lambert W Function

From (3.16)

$$IR_p = I_{\text{ph}} R_p - I_s R_p e^{\frac{V+IR_s}{A_q V_T}} + I_s R_p - V - IR_s \tag{3.29}$$

$$I = \frac{I_{\text{ph}} R_p - I_s R_p e^{\frac{V+IR_s}{A_q V_T}} + I_s R_p - V}{R_p + R_s} \tag{3.30}$$

By multiplying both members for R_s

$$IR_s = \frac{R_s}{R_p + R_s}\left(I_{\text{ph}} R_p - I_s R_p e^{\frac{V+IR_s}{A_q V_T}} + I_s R_p - V\right) \tag{3.31}$$

Then, by adding V to both members,

$$V + IR_s = \frac{R_s}{R_p + R_s}\left(I_{\text{ph}} R_p - I_s R_p e^{\frac{V+IR_s}{A_q V_T}} + I_s R_p - V\frac{R_p}{R_s}\right) \tag{3.32}$$

Now, dividing for $A_q V_T$,

$$\frac{V + IR_s}{A_q V_T} = \frac{R_s}{A_q V_T (R_p + R_s)}\left(I_{\text{ph}} R_p - I_s R_p e^{\frac{V+IR_s}{A_q V_T}} + I_s R_p - V\frac{R_p}{R_s}\right) \tag{3.33}$$

$$\frac{V + IR_s}{A_q V_T} + \frac{I_s R_p R_s}{A_q V_T (R_p + R_s)} e^{\frac{V+IR_s}{A_q V_T}} = \frac{R_s\left(I_{\text{ph}} R_p + I_s R_p - V\frac{R_p}{R_s}\right)}{A_q V_T (R_p + R_s)} \tag{3.34}$$

Taking the exponential of both members

$$e^{\frac{V+IR_s}{A_qV_T}} \cdot \exp\left[\frac{I_sR_pR_s}{A_qV_T\left(R_p+R_s\right)}e^{\frac{V+IR_s}{A_qV_T}}\right] = \exp\left[\frac{R_s\left(I_{\text{ph}}R_p+I_sR_p-V\frac{R_p}{R_s}\right)}{A_qV_T\left(R_p+R_s\right)}\right] \tag{3.35}$$

By multiplying both members for $\frac{I_sR_pR_s}{A_qV_T\left(R_p+R_s\right)}$

$$\frac{I_sR_pR_s}{A_qV_T\left(R_p+R_s\right)}e^{\frac{V+IR_s}{A_qV_T}} \cdot \exp\left[\frac{I_sR_pR_s}{A_qV_T\left(R_p+R_s\right)}e^{\frac{V+IR_s}{A_qV_T}}\right] = \frac{I_sR_pR_s}{A_qV_T\left(R_p+R_s\right)}\exp\left[\frac{R_s\left(I_{\text{ph}}R_p+I_sR_p-V\frac{R_p}{R_s}\right)}{A_qV_T\left(R_p+R_s\right)}\right] \tag{3.36}$$

now, the first member is in the form we^w, then taking the Lambert W of both members:

$$\frac{I_sR_pR_s}{A_qV_T\left(R_p+R_s\right)}e^{\frac{V+IR_s}{A_qV_T}} = \text{Lambert } W\left\{\frac{I_sR_pR_s}{A_qV_T\left(R_p+R_s\right)}\exp\left[\frac{R_s\left(I_{\text{ph}}R_p+I_sR_p-V\frac{R_p}{R_s}\right)}{A_qV_T\left(R_p+R_s\right)}\right]\right\} \tag{3.37}$$

$$I_sR_pe^{\frac{V+IR_s}{A_qV_T}} = \frac{A_qV_T\left(R_p+R_s\right)}{R_s}\text{Lambert } W\left\{\frac{I_sR_pR_s}{A_qV_T\left(R_p+R_s\right)}\exp\left[\frac{R_s\left(I_{\text{ph}}R_p+I_sR_p-V\frac{R_p}{R_s}\right)}{A_qV_T\left(R_p+R_s\right)}\right]\right\} \tag{3.38}$$

The first member can be written by using Eq. (3.16) as:

$$I_sR_pe^{\frac{V+IR_s}{A_qV_T}} = -I\left(R_p+R_s\right)+I_{\text{ph}}R_p-I_sR_p-V \tag{3.39}$$

$$-I\left(R_p+R_s\right)+I_{\text{ph}}R_p-I_sR_p-V = \frac{A_qV_T\left(R_p+R_s\right)}{R_s}\text{Lambert } W\left\{\frac{I_sR_pR_s}{A_qV_T\left(R_p+R_s\right)}\exp\left[\frac{R_s\left(I_{\text{ph}}R_p+I_sR_p-V\frac{R_p}{R_s}\right)}{A_qV_T\left(R_p+R_s\right)}\right]\right\} \tag{3.40}$$

$$I\left(R_p + R_s\right) = -\frac{A_q V_T \left(R_p + R_s\right)}{R_s} \text{Lambert } W\left\{\frac{I_s R_p R_s}{A_q V_T \left(R_p + R_s\right)} \exp\left[\frac{R_s\left(I_{\text{ph}} R_p + I_s R_p - V\frac{R_p}{R_s}\right)}{A_q V_T \left(R_p + R_s\right)}\right]\right\} + I_{\text{ph}} R_p - I_s R_p - V \tag{3.41}$$

$$I = -\frac{A_q V_T}{R_s} \text{Lambert } W\left\{\frac{I_s R_p R_s}{A_q V_T \left(R_p + R_s\right)} \exp\left[\frac{R_s\left(I_{\text{ph}} R_p + I_s R_p - V\frac{R_p}{R_s}\right)}{A_q V_T \left(R_p + R_s\right)}\right]\right\} + \frac{I_{\text{ph}} R_p - I_s R_p - V}{\left(R_p + R_s\right)} \tag{3.42}$$

3.3 Cell-Module/Field

The models described until now have been developed for a single PV cell; however, they can be extended to the case of series/parallel connection of cells inside a PV module or field.

Starting from the double diode model, expressed by Eq. (3.9), an analogous model and equivalent circuit of a PV module/field is obtained provided that a suitable scaling of the parameters is performed. In particular, considering a module/field formed of N_P cells in parallel and N_S cells in series, if solar irradiance and temperature are assumed to be uniform, the following relationships are valid:

$$\begin{cases} I_{\text{ph,tot}} = N_P I_{\text{ph}} \\ I_{\text{tot}} = N_P I \\ V_{\text{tot}} = N_S V \end{cases} \tag{3.43}$$

where the subscript '*tot*' stands for a quantity referred to the whole module or field.

The resulting analytical model is:

$$I_{tot} = I_{\text{ph,tot}} - N_P\left[I_{s1}\left(\frac{q}{e^{A_0 kT}}\left(\frac{V_{\text{tot}}}{N_S} + \frac{I_{\text{tot}} R_s}{N_P}\right) - 1\right) + I_{s2}\left(e^{\frac{q}{2kT}\left(\frac{V_{\text{tot}}}{N_S} + \frac{I_{\text{tot}} R_s}{N_P}\right)} - 1\right) - \frac{\frac{V_{\text{tot}}}{N_S} + \frac{I_{\text{tot}} R_s}{N_P}}{R_p}\right] \tag{3.44}$$

On the other hand, starting from the single diode model expressed by Eq. (3.12), considering the simplification introduced in Eq. (3.13) and with the following positions:

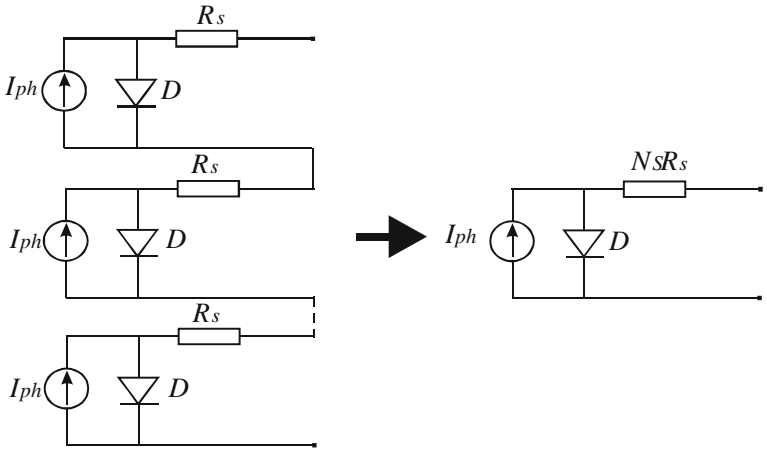

Fig. 3.10 Equivalent circuit model of N_S series connected cells

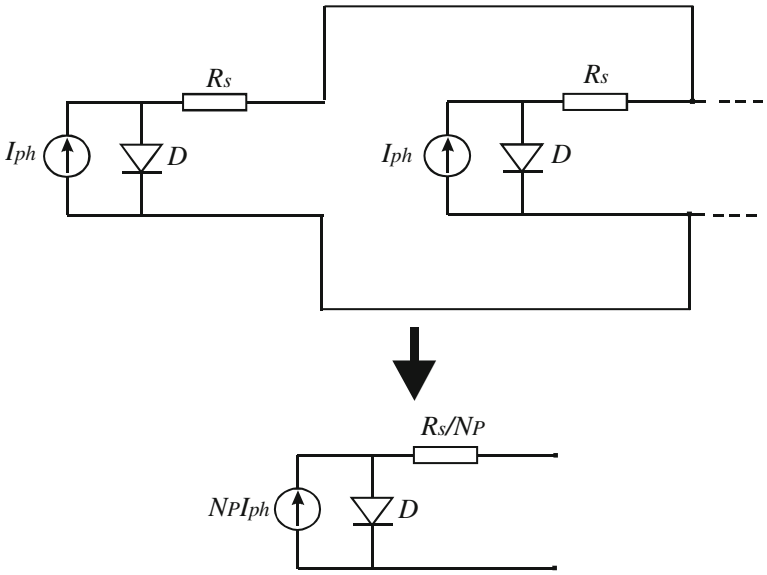

Fig. 3.11 Equivalent circuit model of N_P parallel connected cells

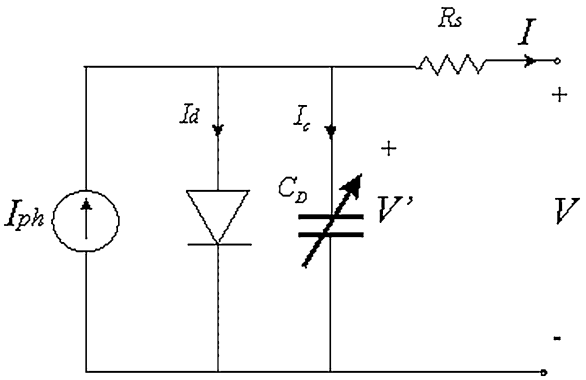

Fig. 3.12 Dynamic circuit model containing nonlinear diffusion capacitance

$$\begin{aligned} I_{\text{ph,tot}} &= I_{0,\text{tot}} \\ \frac{q}{A_q kT} &= K_1 \\ N_P I_s &= e^{K_2} \end{aligned} \tag{3.45}$$

the final expression of the module/field model is:

$$I_{\text{tot}} = I_{0,\text{tot}} - e^{\left[\left(\frac{V_{\text{tot}}}{N_S} + \frac{I_{\text{tot}} R_S}{N_P}\right) K_1 + K_2\right]} \tag{3.46}$$

The equivalent circuit model of the PV module/field can be deduced in this case according to the schemes represented in Figs. 3.10 and 3.11.

3.4 Dynamic Model

The considered models are suited for slow variations of solar irradiance and load. Several situations, however, need a precise knowledge of solar cell behavior during transients. In these cases, a dynamical model is necessary.

3.4.1 Parallel Capacitance

In Sect. 2.12, it has been explained that the *p-n* junction includes a capacitive effect due to the effect of excess minority carriers stored in the quasi-neutral region. This effects can be modeled by a voltage depending capacitance that, for low frequency variations, can be expressed as:

$$C_D = \tau_p \frac{I}{V_T} = \tau_p \frac{I_d}{V_T} e^{b\frac{V'}{V_T}} = C_0 e^{b\frac{V'}{V_T}} \tag{3.47}$$

where C_0 is the so-called base capacitance and b is a fitting parameter.

To consider this dynamic effect in the PV cell model, the variable capacitance, defined by Eq. (3.47), must be included in the circuit model. As a consequence, during transients, a discrepancy between current and voltage obtained by static and dynamic model is expected. This difference depends on the capacitive current I_c that changes the effect of photo-generated current.

The dynamic circuit model containing the nonlinear diffusion capacitance C_D is shown in Fig. 3.12.

For the circuit scheme in Fig. 3.12, the following current balance is valid:

$$I = I_{\text{ph}} - I_d - I_C \tag{3.48}$$

where

$$I_C = \frac{\mathrm{d}}{\mathrm{d}t}(C_D V') = C_D \frac{\mathrm{d}V'}{\mathrm{d}t} + V' \frac{\mathrm{d}C_D}{\mathrm{d}t} \tag{3.49}$$

using (3.47)

$$\frac{\mathrm{d}C_D}{\mathrm{d}t} = C_0 \frac{b}{V_T} e^{b\frac{V'}{V_T}} \tag{3.50}$$

Therefore,

$$I_C = C_0 e^{b\frac{V'}{V_T}} \left(b\frac{V'}{V_T} + 1 \right) \frac{\mathrm{d}V'}{\mathrm{d}t} \tag{3.51}$$

Finally, taking into account that $V' = V - IR_S$, the expression of the capacitive current versus electrical parameters measured at the PV cell terminals can be achieved.

$$I_C = C_0 e^{b\frac{(V-IR_S)}{V_T}} \left(b\frac{V - IR_S}{V_T} + 1 \right) \frac{\mathrm{d}(V - IR_S)}{\mathrm{d}t} \tag{3.52}$$

if the variation of the external voltage V is negligible, the following equation is obtained:

$$I_C = -R_S C_0 e^{b\frac{(V-IR_S)}{V_T}} \left(b\frac{V - IR_S}{V_T} + 1 \right) \frac{\mathrm{d}I}{\mathrm{d}t} \tag{3.53}$$

By Eq. (3.53) it is possible to notice that the nonlinear junction capacitance influences the current balance in Eq. (3.48) with a term proportional to the series resistance and the base capacitance that is relevant only when a fast load current variation occurs. Finally, being this capacitance parallel connected to the diode and the current generator, when N_S cells are series connected, the capacitance equivalent value is divided by N_S.

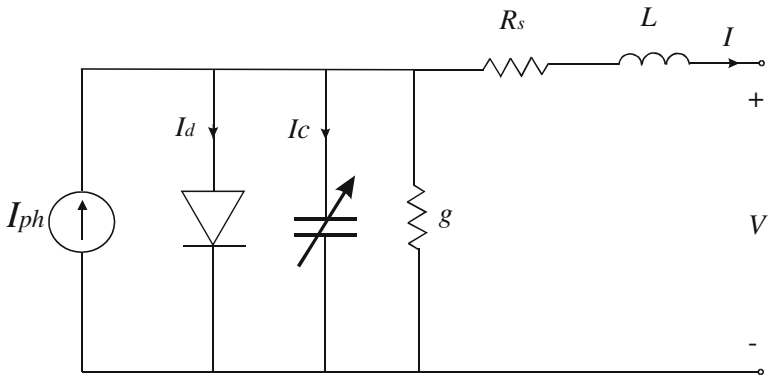

Fig. 3.13 Dynamic circuit model containing nonlinear diffusion capacitance and parasitic inductance

3.4.2 Series Inductance

For sudden photovoltaic current or load variation at first instants, time domain waveforms of external voltage and current may differ from those obtained by the model described in Sect. 3.4.1. This is due to both the facts that for fast variations a more complicated capacitance model should be used, as explained in 2.12, for high frequencies and to the presence of a low parasitic inductance of electrical wires connecting the cell to the electric terminals.

The dynamic circuit model containing nonlinear diffusion capacitance and parasitic inductance is shown in Fig. 3.13. When N_S cells are series connected, the parasitic equivalent inductance is multiplied by N_S.

3.5 Modeling PV Fields under Nonuniform Illuminating Conditions

As previously stated, the PV modules are composed of matrices of solar cells interconnected in series and parallel and PV fields are given by a set of series/parallel connected modules.

The overall electrical characteristic of a PV field is obtained by the composition of the electrical characteristics of its modules.

Figures 3.14 and 3.15 schematize, for the case of two identical modules under the same solar irradiance, the composition process used to obtain the *I*–*V* characteristic of the PV field, from the knowledge of the *I*–*V* characteristics of the modules.

The overall series connection *I*–*V* curve is obtained by summing the voltage point-by-point for each value of the common current. As a result, the open circuit voltage is twice the open circuit voltage of the single module.

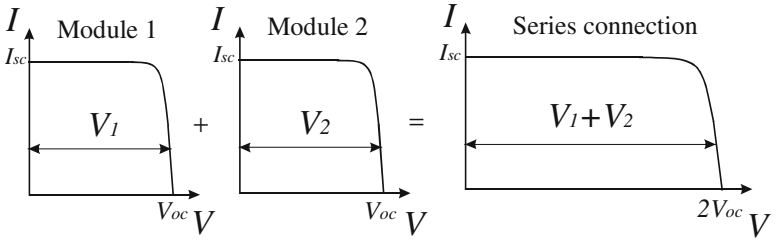

Fig. 3.14 Composition of *I–V* curves for series connected modules under the same solar irradiance in a PV field

Fig. 3.15 Composition of *I-V* curves for parallel connected modules under the same solar irradiance in a PV field

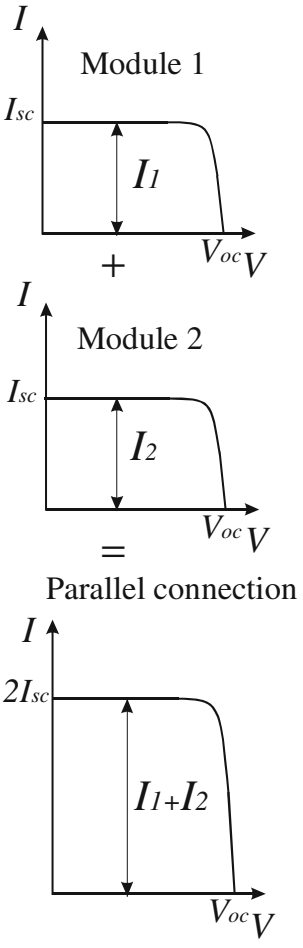

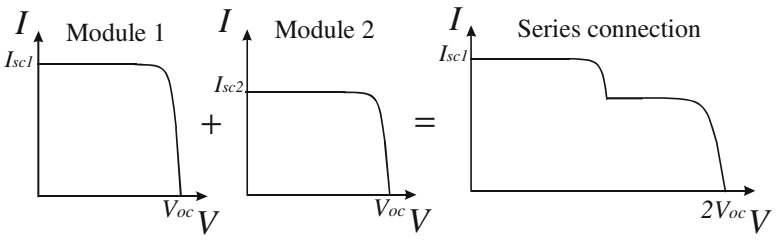

Fig. 3.16 Composition of *I–V* curves for two series connected modules under different solar irradiance in a PV field

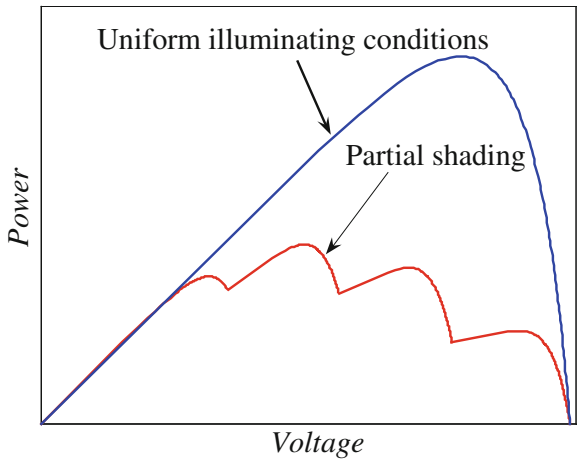

Fig. 3.17 Comparison between *P–V* curves under uniform and nonuniform irradiance

The process can be obviously extended to the case of PV field formed of an arbitrary number of series/parallel connected modules.

In the case of PV modules under different solar irradiance, the shape of the overall *I–V* curve shows steps that correspond to the occurring of local maxima in the power-voltage (*P–V)* curve, as will be explained in the following. Figure 3.16 illustrates the composition process when two modules are series connected and subject to different solar irradiance. The series connection is the most frequent case encountered when dealing with PV fields, since a high output voltage is often necessary to supply the electrical load.

When more modules are series connected, and they operate under different solar irradiance, the definition of the whole PV field characteristics is obtained by summing the single contributions.

As a matter of fact, the PV field performance is dependent on the behavior of the individual solar cells and this could be critical, especially in nonideal operating conditions.

An usual nonideal operating condition that strongly affects PV field during electric generation is the partial shading, i.e., the non-uniform distribution of the

solar irradiance on the PV field surface. This problem is mainly due to clouds passing over a portion of the PV array and is particularly serious for large installations.

Partial shading leads to a reduction of the available output power. Moreover, the occurrence of multiple local maxima in the P–V characteristic, due to non-uniform solar irradiance, can cause a failure of the MPPT control with a relevant power loss due to the lack of the real MPP detection. Figure 3.17 illustrates the qualitative difference between P–V characteristics of PV field under uniform illuminating conditions and under partial shading.

It is evident that the correct determination of solar irradiance distribution over a PV array is crucial both for the optimization of the MPPT strategy and for a correct prediction of the PV system energy capability.

Usually, manufacturers give the characteristic parameters referred to a photovoltaic module supposed under uniform solar irradiance and temperature; hence, it is useful to obtain the model of the modules and to build the whole characteristic of the PV field on the basis of their electrical connections.

Depending on the design and the dimensions of the considered PV field, the best approach could be to separate its model into single modeling units (the modules), as solar irradiance and temperature are unlikely to change across the dimensions of a single unit, while they could possibly change across the dimensions of the whole field. In this way each module can be characterized on the basis of its own temperature and solar irradiance, so partial shading situations and other nonideal operating modes can be investigated, as well as the case of uniformly illuminated PV field.

To be more precise, once the module I–V characteristics are available, a composition process is necessary to characterize the whole PV field. This process is based on:

- the sum of module voltages, the currents being equal, for series connected modules;
- the sum of currents, the voltages being equal, for parallel connected modules.

In order to avoid possible mismatch in series or parallel connection, in a real installation, *bypass* and *block* diodes are provided.

The bypass diodes are used to protect series connected modules from problems due to possible current mismatch.

The block diodes are used to avoid that, under some operating or fault conditions, a string, i.e., the series connection of modules, could be interested by a reverse current generated by other strings.

The installation and the usefulness of such diodes are described by Fig. 3.18.

As for the *bypass* diode, it is parallel connected to each module in the PV field, as shown in Fig. 3.18a. When a module is completely shaded, it operates in the point $I \approx 0, V \approx 0$ and does not allow the current coming form other modules to flow. The *bypass* diode, in this case, give an alternative way to the current. When the module is illuminated, the *bypass* diode is inverse polarized and behaves as an open circuit.

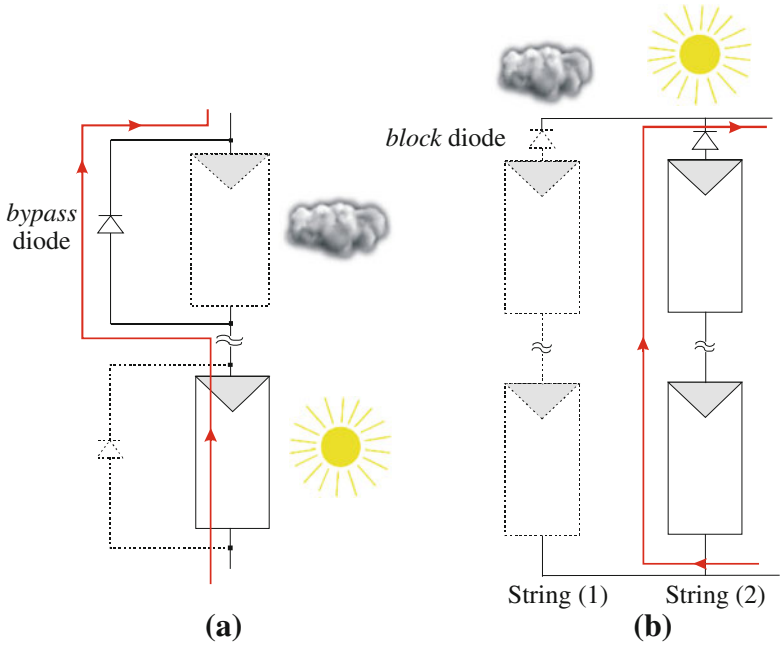

Fig. 3.18 Installation and operation of *bypass* diode (**a**) and *block* diode (**b**)

As for the *block* diode, it is series connected to a PV string, as shown in Fig. 3.18b. With reference to Fig. 3.18b, when the string (1) is partially shaded, its voltage is lower than the voltage of string (2). The *block* diode is inverse polarized and prevents string (1) from imposing its low voltage to the parallel of the two strings. On the other hand, the *block* diode causes a power loss equal to the product of the threshold voltage of the diode and the direct current ($V_{\text{threshold}} \cdot I$) and must be able to undertake a reverse voltage equal to the open circuit voltage of the string and a forward current equal to the maximum current delivered by the string.

Several configurations, in terms of modules connection and conditioning power electronics, have been proposed in the last decade in the field of PV grid connected plants, starting from centralized architectures to more and more decentralized technologies. Some examples of modules configurations used in real PV plant, in particular, the centralized technology, the string and multi-string technology, and the AC module technology are represented in Fig. 3.19. In the schemes of Fig. 3.19 the *bypass* and *block* diodes are not sketched, for the sake of simplicity.

Figure 3.19 represents the evolution of PV plants from the past (left) to the future (right). In particular, in Fig. 3.19a, a centralized inverter configuration is drawn. This kind of plant is the oldest realization to inject power coming from PV modules into the grid. The source is realized by series connection of PV modules to obtain a high voltage that supplies directly the inverter stage. This power stage was a line commutated inverter with thyristors as power switch. Among disadvantages

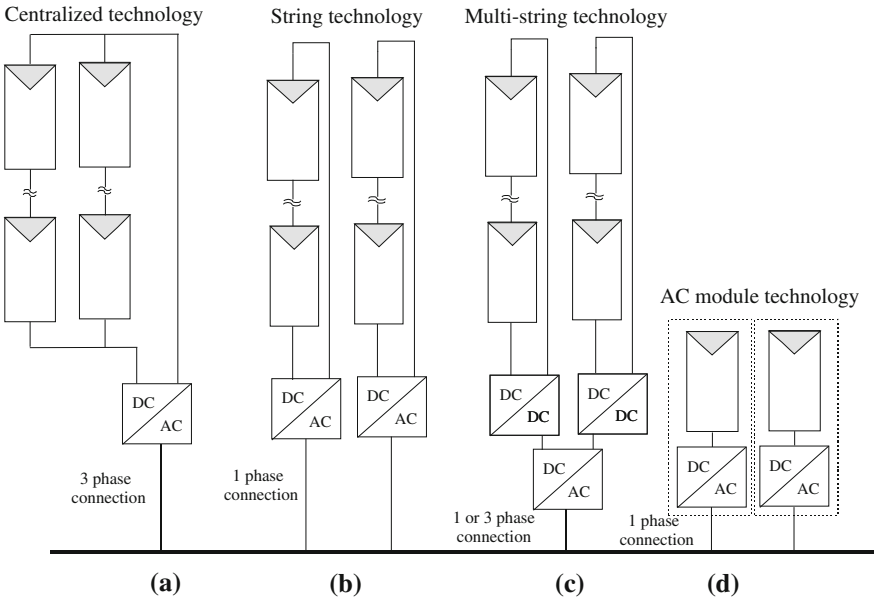

Fig. 3.19 Examples of module configurations in PV grid connected plants: centralized technology (**a**), string technology (**b**), multi-string technology (**c**), AC module technology (**d**)

there are: the high voltage of DC cables at the inverter input, the need of blocking diodes at the end of the strings, and the poor quality of power injected to the grid.

Figure 3.19b shows a more recent system in which each string is connected to a dedicated single-phase inverter. In this case there is no need of blocking diode, the input inverter voltage can be reduced by adopting a step-up transformer before the connection to the grid. In this configuration each inverter can perform a maximum power point tracking (MPPT) on its string and, compared to the centralized inverter, a greater efficiency is achieved and the system exhibits a better modularity.

Figure 3.19c shows a multi-string technology realization. Each string is connected to a DC/DC converter that performs the MPPT and raises the input voltage of the inverter. The system can be extended by adding new strings with its own DC/DC stage if the inverter is correspondingly designed.

Finally, in Fig. 3.19d the AC module technology is shown. In this case each module is connected to a DC/AC stage that boosts the module voltage, performs the MPPT, and the grid connection; no by-pass diodes are necessary.

The evolution, during the time, from (a) to (d) plants has been made possible thanks to the evolution of power devices as MOSFETs and IGBTs that have been exhibiting high blocking voltages, high conduction currents with fast commutation times.

3.6 Conclusions

An overview of mathematical models of PV sources and the corresponding derivation of equivalent circuits have been given in this chapter. Both the mathematical model and the circuit model are the basis for the PV source behavior reproduction.

Starting from a nearly ideal behavior of a PV cell, the different nonideality elements, related to the operation of a real PV device, have been included in the model. Furthermore, from a generalized PV model, some simplifications, valid when dealing with electric power generation, have been introduced.

The extension of PV cell model to the case of PV modules or fields has been presented, and finally some issues related to the use of the models under non-uniform solar irradiance have been outlined.

It should be observed that the advantageous use of the previously described models is possible only if a suitable extraction of their parameters is done. For this reason, the parameters identification is a crucial stage in the setup of a precise and reliable PV model.

The methods for the extraction of the PV model parameters will be the object of following two chapters, the former dedicated to the case of static models and the latter focused on the case of dynamic models.

Bibliography

Castañer L, Silvestre S (2002) Modelling photovoltaic systems using Pspice. Wiley, Chicester

Chan SH, Phang JCH (1987) Analytical methods for the extraction of solar-cell single-and double-diode model parameters from I-V characteristics. IEEE Trans Electron Devices ED-34(2): 286–293

Di Piazza MC, Vitale G (2010) Photovoltaic field emulation including dynamic and partial shadow conditions. Appl Energ (87)3: 814–823

Gow JA, Manning CD (1999) Development of a photovoltaic array model for use in power-electronics simulation studies. IEE Proc Elect Power Appl 146(21):193–200

Gradella Villalva M, Gasoli JR, Filho ER (2009) Comprehensive approach to modeling and simulation of photovoltaic array. IEEE Trans Power Electron 24(5):1198–1208

Luque A, Hegedus S (eds) (2003) Handbook of photovoltaic science and engineering. Wiley, Hoboken

Messenger RA, Ventre J (2005) Photovoltaic systems engineering, 2nd edn. CRC Press, Boca Raton

Sera D, Teodorescu R, Rodriguez P (2007) PV panel model based on datasheet values. IEEE Intern Symp Ind Electron 2392–2396

Kjaer SB, Pedersen JK, Blaabjerg F (2005) Review of single-phase grid-connected inverters for photovoltaic modules. IEEE Trans Ind Appl 41(5):1292–1306

Friesen G, Ossenbrink HA (1997) Capacitance effects in high-efficiency cells. Solar Energ Mater Solar Cells 48: 77–83

Jain A, Kapoor A (2005) A new approach to study organic solar cell using Lambert W-function. Solar Energ Mater Solar Cell 86:197–205